*Acta Cryst.* (1964). **17**, 1437

# Ice II: A Proton-Ordered Form of Ice*

By Barclay Kamb

*Division of the Geological Sciences, California Institute of Technology, Pasadena, California, U. S. A.*

(*Received* 5 *August* 1963)

Ice II, one of the high-pressure polymorphs of ice, of density 1·17 g.cm$^{-3}$, has $12H_2O$ molecules in a rhombohedral unit cell with $a = 7{\cdot}78$ Å, $\alpha = 113{\cdot}1°$. According to the Laue symmetry shown in single-crystal photographs, the space group should be either $R\bar{3}m$, $R3m$ or $R32$. Centrosymmetry is indicated by a statistical test with essentially three-dimensional intensity data. However, the Patterson function indicates a pseudo-structure in space group $R\bar{3}c$. The true structure must be appreciably distorted from this because of moderately strong violation of the *c*-glide extinction condition. The distortion could degrade the space group to $R32$, but the resulting structure has unsatisfactory features, and does not conform well with the experimental data. Structural reasoning indicates space group $R\bar{3}$. The observed $R\bar{3}m$ Laue symmetry must therefore be the result of intimate twinning of $R\bar{3}$ individuals. The structure in $R\bar{3}$ can be refined, under the assumption of twinning, and with the inclusion of hydrogen atoms, to $R = 0{\cdot}08$.

The basic $R\bar{3}c$ structure contains ice-I-like units built out of puckered 'six-rings' of water molecules. These units are linked together in a more compact way than in ice I. Each oxygen atom is bonded to four nearest neighbors at $2{\cdot}80 \pm 0{\cdot}04$ Å, and has in addition a next-nearest neighbor at 3·24 Å. The distortion of the true structure from the pseudo-structure leaves the bond lengths essentially unaltered but changes the bond angles appreciably. It constitutes evidence that the hydrogen atoms are in ordered arrangement in the crystal, rather than disordered, as in ice I. The particular ordered arrangement actually realized can be deduced from detailed features of the structure. This arrangement gives better agreement with the X-ray data than any other, although the X-ray distinction among various arrangements is necessarily marginal.

The ordering energy in ice II, formulated in terms of the H-bond strain, must involve significantly the effects of both donor- and acceptor-misorientation. The acceptor strain energy contribution is found to depend primarily not on deviation from tetrahedral bond orientation relative to the accepting $H_2O$ but on deviation from the 'accepting plane' that bisects the H–O–H angle of the molecule. The $H_2O$ environment in ice II deviates greatly from an ideal tetrahedral one, yet the H-bond strain energy, although greater than in ice I, is small enough to be offset by the extra van der Waals energy, so that the energy of ice II is only 0·01 kcal.mole$^{-1}$ greater than that of ice I. The measured entropy difference between I and II is a direct reflection of the entropy of proton-disorder in ice I.

## Introduction

Ever since Pauling's fruitful proposal (1935) that the protons in ice are in a disordered arrangement, the idea of proton disorder has played an important part in interpreting the structure and physical properties of ice and related substances. Careful studies of the ice I structure (Peterson & Levy, 1957; see also Lonsdale, 1958, and Owston, 1958) have failed to reveal any sign of ordered proton arrangements such as the ones proposed originally by Bernal & Fowler (1933), and a theoretical attempt to demonstrate that proton ordering is favored energetically (Bjerrum, 1952) has proved faulty (Pitzer & Polissar, 1956).

It now appears, however, that there is a high-pressure ice polymorph, ice II, in which the protons are ordered. The present paper presents the evidence for this conclusion, based on a determination of the ice II structure. It is part of a systematic study of the crystal structures of the high-pressure forms of ice, of which the results for ice III have been reported previously (Kamb & Datta, 1960*a*, *b*).

The six high-pressure forms of ice are produced at pressures upwards of 2000 atmospheres; their various fields of stability were determined by Bridgman (1912, 1935, 1937). Ice II, the form of interest here, occupies the lowest-temperature portion of the *P*, *T* field investigated by Bridgman, as shown in Fig. 1. The structure of ice II was studied by McFarlan (1936*a*, *b*) using X-ray powder diffraction methods; however, as reported previously (Kamb & Datta, 1960*a*, *b*), the structure found is not a plausible one and the powder data on which it is based are not those proper to ice II.

## Experimental

The experimental technique used for preparing the high-pressure ice samples and investigating them by

* Contribution No. 1197 from Division of the Geological Sciences.

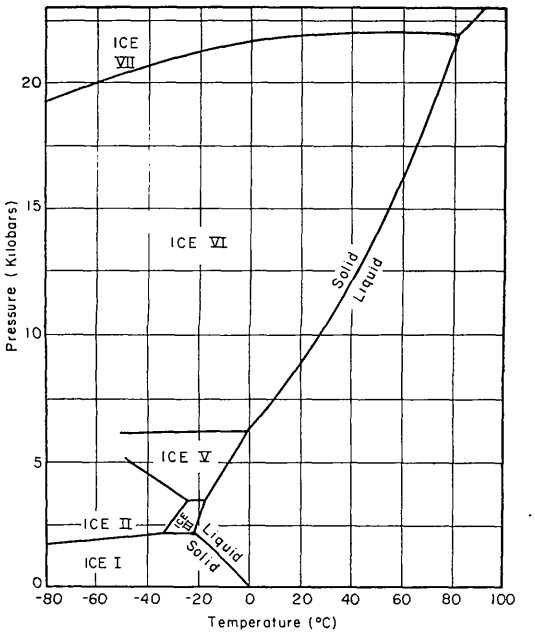


Fig. 1. Phase diagram of the $H_2O$ system, after Bridgman (1912, 1937). Solid phases are numbered from I to VII (IV omitted).

X-ray diffraction has been described in connection with the results for ice III (Kamb & Datta, 1960*c*); it was used without essential modification here. Preparation of ice II is accomplished by cooling a water sample at low pressure to −75 °C, and then raising the pressure to about 3000 atmospheres. At pressures below about 3000 atmospheres the rate of transformation is too slow to get a consistent yield of ice II, and at pressures above 3500 atmospheres (at −75 °C) a different phase is formed, which has not yet been identified. At temperatures much above about −70 °C but still within the ice II stability range, ice III forms metastably instead of ice II. Identification of ice II as the phase formed in the way described was discussed by Kamb & Datta (1960*c*); this identification has been confirmed recently by Bertie, Calvert & Whalley (1963).

The density of ice II was not measured directly but was determined by comparison with ice III, in the following way. Needed is the density under the conditions of X-ray observation: atmospheric pressure and −150 °C. From the known structure of ice III its density under the pertinent conditions is calculated to be 1·141 g.cm$^{-3}$. At the triple point ice I — ice II — ice III, the difference in specific volume between III and II (Bridgman, 1912, p. 524) is $V(\text{III})-V(\text{II})=0{\cdot}021$ cm$^3$.g$^{-1}$. The alteration of this volume difference in going from the triple point, at $P=2{\cdot}1$ kbar, $T=-22$ °C, to the conditions $P=1$ bar, $T=-150$ °C is estimated by assuming that both II and III have a compressibility over the pressure range 0 to 2·1 kbar equal to that determined for III over the range 2 to 3·5 kbar by Bridgman (1912, p. 535), and by assuming that they have the same coefficient of thermal expansion as that of ice I, which has been evaluated by Lonsdale (1958). The inaccuracies involved in these assumptions are not serious, because the volume difference is small compared with the specific volumes themselves. The density of ice II obtained is 1·170 g.cm$^{-3}$.

## X-ray data

Because ice II forms only by transformation from other solid phases (Fig. 1), it had been expected that the product would be a fine-crystalline powder unsuited for single-crystal study. This was suggested also by McFarlan's early observations (1936*b*, pp. 84–85). However, single crystals or coarse aggregates of a few crystals formed with fair frequency in the glass capillaries used. The crystals proved to be easier to study than crystals of ice III, because ice II does not show the spontaneous inversion under X-irradiation that was found for ice III (Kamb & Datta, 1960*c*).

The unit cell of ice II is rhombohedral, with $a_R=7{\cdot}78\pm0{\cdot}01$ Å, $\alpha=113{\cdot}1\pm0{\cdot}2°$; the corresponding triply-primitive hexagonal cell has $a_H=12{\cdot}97\pm0{\cdot}02$, $c_H=6{\cdot}25\pm0{\cdot}01$ Å. These values were determined from precession photographs with Cu $K\alpha$ radiation of assumed wavelength $\lambda=1{\cdot}542$ Å.* The Laue symmetry shown is $\bar{3}m$, and there are no systematic extinctions. The space group indicated should, therefore, be one of the three $R\bar{3}m$ ($D_{3d}^5$), $R32$ ($D_3^7$), $R3m$ ($C_{3v}^5$).

Two single crystals suitable for collecting quantitative diffraction data were found in the course of the work, and from these a nearly complete three-dimensional set of data was obtained by precession and rotation methods. The set of photographs available for intensity measurement is shown in Table 1. The rotation photographs were obtained with the precession camera by setting the precession angle to zero and turning the spindle axis at constant rate.

Table 1. *X-ray data for ice II*

The table lists the number of photographs of each type used in the intensity measurements

| Method | Reflection type* | Radiation Cu $K\alpha$ | Radiation Mo $K\alpha$ |
|---|---|---|---|
| Precession | $hk0$ | 1 | 2 |
| | $hk1$ | 1 | 2 |
| | $hk2$ | 0 | 1 |
| | $hhl$ | 1 | 0 |
| | $hk(2k-h)$ | 1 | 0 |
| | $hk(2k-h+1)$ | 1 | 0 |
| | $hk(2k-h+2)$ | 1 | 0 |
| Rotation ($c_H$ axis) | $hkl$ | 2 | 3 |

* Rhombohedral indices.

* Bertie *et al.* (1963) have recently reported a unit cell determination for ice II, obtained by methods very similar to those used here, and in agreement with the above results.

The number of reciprocal planes photographed by the precession method was limited by accidental loss of the crystals. The precession photographs intercept 252 out of the approximately 600 non-equivalent reciprocal lattice points out to $\sin\theta/\lambda = 0{\cdot}7$. 142 reflections were strong enough to be observed. The rotation photographs record all points out to $\sin\theta/\lambda = 0{\cdot}57$, except for a few points close to the $c_H$ axis. There are approximately 320 non-equivalent points within this limit. 86 reflections were actually observed, of which 22 are subject to ambiguity in indexing because they can represent superimposed pairs (rarely, triplets or quadruplets) of non-equivalent reflections. With the help of the precession data it was possible to resolve all but 3 of these ambiguities. The rotation data contain only 13 observed reflections that are not present in the precession set of data; 3 of these 13 are unresolvable pairs. It is thus seen that the intensity data are essentially three-dimensional as far as strong and moderate reflections are concerned.

Intensities were estimated visually in the usual way, from the photographs listed in Table 1, and were corrected for the Lorentz and polarization effects. The precession data were then reduced to a common scale, as were also, separately, the rotation data. No absorption corrections for the Cu $K\alpha$ data were applied, as none appeared to be indicated by comparisons with the Mo $K\alpha$ data. Scaling of the precession planes to one another is facilitated by the rhombohedral symmetry. Rotation intensities were corrected by the appropriate multiplicities.

Comparison between the precession data and the rotation data indicated a considerably larger uncertainty in the estimate of the relative scaling factor than had been found for the within-group scaling comparisons. When the logarithmic intensity differences for reflections common to the two sets of data were plotted against $\sin\theta$, a well-defined linear regression resulted, about which the scatter was comparable to that shown in the within-group scaling comparisons. This effect is thought to be due to an incipient splitting of the individual reflections that is observable in the rotation photographs. The splitting is attributed to a coarse mosaic containing rather widely diverging crystal orientations, since it could not be eliminated by careful alignment of the crystals. The splitting causes a spreading out of the reflection spots which increases progressively with $\sin\theta$; it is most severe on the higher layer lines ($l_{\text{hex}} = 4$ and 5). The subjective technique of visual intensity estimation tends more to measure peak photographic density than integrated density, apparently, and hence the splitting leads to a progressive decrease in the estimated rotation intensities as a function of $\sin\theta$, relative to the precession intensities for which the splitting effect is less strong. This interpretation is supported by the fact that the regression lines obtained separately for the Cu $K\alpha$ rotation photographs and the Mo $K\alpha$ rotation photographs have almost the same slope if plotted against $\sin\theta$, but not against $\sin\theta/\lambda$.

On this basis, the rotation data were scaled to the precession data by applying corrections obtained from the linear regression line. The sets of data from all photographs on a common scale were then averaged, and the intensities of reflections involved in superimposed pairs in the rotation photographs were obtained by difference where possible. The complete set of data contains 152 observed reflections, 3 unresolved pairs, and 126 reflections weaker than a known limit of observation.

## Structure determination

The density and cell dimensions indicate that the unit cell of ice II contains 12 water molecules. The density calculated on this basis is 1·17 g.cm$^{-3}$, in complete agreement with the density value estimated from experimental measurements.

From the cell dimensions and content, two possible structures can be constructed that give plausible interatomic distances and coordination relationships among the water molecules. One structure is an analog of the silicate framework in the mineral sodalite, distorted from cubic to rhombohedral symmetry. An $H_2O$ framework of the sodalite type occurs in the hydrate $HPF_6 . 6H_2O$ (Bode & Teufer, 1955). The other structure has no analog among silica or silicate structures, but may nevertheless be described as a framework structure involving tetrahedral linkages. However, neither of these structures is in a space group proper to ice II, the first because of body centering corresponding to a smaller primitive cell in space group $R3m$, and the second because of a $c$ glide plane, the space group being $R\bar{3}c$.

Because these discrepancies appeared unavoidable for the *a priori* structures, a direct structure determination was undertaken. The intensities were put on an absolute scale by means of a Wilson plot. A zero-moment test (*International Tables for X-ray Crystallography*, 1959, p. 357) showed clear centrosymmetry for the structure, indicating the space group $R\bar{3}m$. The three-dimensional Patterson function was calculated, using a Burroughs 220 program written by K. Hoogsteen.

The Patterson function indicates that each oxygen atom has four nearest neighbors, at distances of $2{\cdot}81 \pm 0{\cdot}03$ Å. In spite of the indicated space group $R\bar{3}m$, there are no vectors of the type $(X, X, 0)$ required by the operation of the mirror plane. Instead, there are three non-equivalent vectors of the type $(X+\frac{1}{2}, \bar{X}+\frac{1}{2}, \frac{1}{2})$, suggesting a $c$ glide plane. Because of the contradictory indications, a method was sought that would define the structure independently of the assumed space group. This can be done by utilizing the threefold symmetry axis. Only one vector of the type $(X, Y, -X-Y)$ required by the operation of

this axis is present, and it defines the positions of all of the oxygen atoms in $c_H$-axis projection. A nearest neighbor vector (length 2·84 Å) is related to the $(X, Y, -X-Y)$ vector in such a way as to generate a puckered hexagonal ring (symmetry $\bar{3}$) of six oxygen atoms; there must be two such rings in the structure. Application of the vectors of type $(X+\frac{1}{2}, \bar{X}+\frac{1}{2}, \frac{1}{2})$ leads to a placing of the rings relative to one another in the cell, and the resulting structure accounts for all of the remaining Patterson vectors.

The structure so determined is in space group $R\bar{3}c$, and is equivalent to the second *a priori* structure mentioned above. It involves a single 12-fold oxygen position (12*f* in $R\bar{3}c$). With coordinates derived from the Patterson vectors, and an isotropic temperature parameter from the Wilson plot, a structure factor calculation for this structure gives a good overall pattern of agreement ($R=0{\cdot}30$) with the observed structure amplitudes, except for the *c*-glide extinctions that are predicted.

The absence of these extinctions requires that the actual structure differ by some perturbation from the pseudo-structure in $R\bar{3}c$. The perturbation must affect the oxygen positions and must be appreciable, since it can be shown that no arrangement of the hydrogen atoms could account for more than a small fraction of the amplitude of reflection 111, which is one-third of the largest observed for all reflections.

A measure of the required perturbation can be obtained by carrying out a Fourier synthesis in which the structure is treated as though it were in $R\bar{3}c$, using the signs of the structure factors calculated previously and omitting the *hhl* reflections with *l* odd. This calculation gives in some sense an 'average' structure obtained by superposing upon the actual structure the structure generated from it by carrying out a *c*-glide operation. It is found that the peak representing the single oxygen atom in the $R\bar{3}c$ structure is elongated in a certain direction in the crystal. This elongation can be interpreted as a 'splitting' of the single oxygen atom into two unresolved half-atoms. From the shape of the elongated peak the magnitude of the splitting between the half atoms can be estimated, and thus the perturbation vector determined. The splitting can be controlled also by the amplitude of the 111 reflection. It amounts to 0·25 Å.

The way in which the perturbation vector is to be applied to the $R\bar{3}c$ structure to get the actual structure depends on the space group of the latter. The most obvious choice for this is $R32$, which is the only space group in Laue group $\bar{3}m$ obtainable from $R\bar{3}c$ by dropping the *c* glide plane. The resulting structure has unsatisfactory features, however. The puckered six-rings of oxygen atoms become distorted so that the O–O distances within them are not all equal. The two rings remain equivalent, related by the twofold axis, but their relative position shifts in the cell so that they are unequally bonded to one another on opposite sides. The nearest-neighbor distances on one side of the ring become 3·01 Å, and on the other side 2·57 Å. The distance 2·57 Å is almost certainly too short to be acceptable as a hydrogen-bond distance in ice.

Strong experimental evidence against the $R32$ structure is provided by the *hhl* reflections having *l* odd, which are sensitive to the way in which the perturbation vector is applied. There are 28 reflections of this type in the data list, of which 11 were observed. An immediate test of the $R32$ structure is not possible, because experience shows that, with the exception of 001, all of these reflections are sufficiently sensitive to the oxygen positions that meaningful conclusions can be drawn from the structure amplitude agreement for refined structures only. In a least-squares refinement of the $R32$ structure accordingly carried out, for which the overall structure amplitude agreement converged to $R=0{\cdot}17$, the pattern of agreement for the *hhl* reflections with *l* odd remained poor. It corresponds to a residual $R=0{\cdot}46$ figured by including in addition to the 11 observed reflections the 4 unobserved reflections for which $|F_c|$ is greater than the limits of observation, which were assigned as the $|F_o|$ values in these cases. This residual is to be compared with 0·17 for the correct structure.

Another type of structural argument, given later, indicates that the actual space group must lack the twofold axis contained in $R\bar{3}c$. There is, however, no way to drop both the *c* glide and the twofold axis in $R\bar{3}c$ while remaining in Laue group $\bar{3}m$. This leads to the conlucion that the true Laue group must be $\bar{3}$, and that the apparent Laue symmetry $\bar{3}m$ shown in the X-ray photographs is produced by a twinning of $R\bar{3}$ individuals. The scale of this twinning must be fine enough to give essential equality of intensities of '*hkl*' and '*khl*' reflections obtained by superposition of *hkl* and *khl* intensities from equal volumes of untwinned and twinned domains, and yet it must be coarse enough that no diffuseness of the *hhl* reflections with *l* odd is observed.

If the perturbation vector is accordingly applied in $R\bar{3}$, a structure results in which the two puckered six-rings are non-equivalent but in which all nearest-neighbor distances are close to 2·80 Å. This structure can be tested against the observed data, under the assumption of twinning, by comparing $G_c \equiv [\frac{1}{2}F_c^2(hkl)+\frac{1}{2}F_c^2(hkl)]^{\frac{1}{2}}$ against $G_o(hkl)$. The agreement residual is $R=0{\cdot}14$ before any further refinement of the structure.

The space group $R3$ is also possible, but the single perturbation vector derived in the way described provides insufficient information to generate a structure in this space group. The zero-moment-test indication of centrosymmetry cannot be applied to distinguish between $R\bar{3}$ and $R3$, because it is dominated by the pseudo-space-group $R\bar{3}c$. Structural reasoning,

given later, does not support a structure in $R3$, and no attempt was made to derive a set of oxygen positions for refinement in this space group.

### Refinement of the structure

Least-squares refinement of the $R\bar{3}$ structure was carried out with a weighted sum of residuals of the form $\Sigma w[2G_o^2(hkl)-F_c^2(hkl)-F_c^2(khl)]^2$. The program for doing this is a modification of the triclinic least-squares program written by R. E. Marsh for the Burroughs 220 computer. The modified program calculates and solves the full $6\times6$ matrix of least-squares coefficients for the positional coordinate shifts of the two non-equivalent oxygen atoms in the $R\bar{3}$ structure. Inclusion of all off-diagonal terms in the matrix is necessary because the two atoms interact strongly in their contributions to most of the reflections, owing to the pseudo-symmetry and the twinning.* The refinement reduced the structure amplitude residual to $R=0{\cdot}11$ for the 152 observed reflections.

To test the sensitivity of the data to contributions from the hydrogen atoms, which had not been included up to this point, structure factor calculations were made for various proton arrangements: (1) the eight ordered arrangements in space group $R\bar{3}$ that involve only one proton per O · · · O bond; (2) several ordered arrangements in $R\bar{3}$ that violate this requirement; (3) the proton-disordered arrangement, also in $R\bar{3}$; (4) several ordered arrangements in $R3$. In these calculations the oxygen parameters were held fixed, the scale factor and oxygen temperature factor having been first adjusted to fit the inclusion of hydrogen atoms. For simplicity the protons were placed on the center lines between oxygen atoms, distant 1·0 Å from the appropriate centers; this is not exactly correct, because the oxygen coordination polyhedra are distorted from ideal tetrahedral shape, but it probably introduces no significant error.

* The weighting function chosen varies inversely as $G_o^2$ for $G_o>10{\cdot}0$, and assigns unit weight to all residuals for which $G_o$ lies between 10·0 and the limit of observation, which ranges from about 2·0 to about 7·5 over the range of observational conditions involved. The constant-weight portion of the function was used to avoid overemphasis on intensities near the limit of observation, where the accuracy of intensity estimation is inherently poorer than at higher levels. The $G_o^{-2}$ function was used instead of $G_o^{-1}$ to avoid instabilities that experience shows can arise with the latter weighting function (R. E. Marsh, personal communication). Unobserved reflections were included with unit weight when $G_c$ was greater than the limit of observation, which was assigned as the $G_o$ value in such cases.

Table 2. *Observed and calculated structure amplitudes**

$$G_c=[\tfrac{1}{2}F_c^2(hkl)+\tfrac{1}{2}F_c^2(khl)]^{\frac{1}{2}}$$

| $h\,k\,\ell$ | $G_o$ | $G_c$ |
|---|---|---|
| $0\,\bar{9}\,9$ | < 3.8 | 2.8 |
| $8\,\bar{8}\,8$ | < 4.4 | 0.4 |
| $\bar{9}\,9\,9$ | < 4.0 | 1.0 |
| $\bar{7}\,7$ | 9.3 | 9.7 |
| 8 | 4.9 | 4.5 |
| 9 | 4.2 | 2.7 |
| $\bar{10}$ | 1.9 | 1.2 |
| $\bar{6}\,6$ | 6.6 | 6.6 |
| 7 | 4.1 | 2.2 |
| 8 | 5.5 | 5.2 |
| 9 | 4.3 | 4.9 |
| $\bar{10}$ | 1.4 | 2.7 |
| $\bar{5}\,5$ | 9.3 | 7.7 |
| 6 | 4.6 | 4.2 |
| 7 | < 4.3 | 1.1 |
| 8 | < 4.5 | 3.4 |
| 9 | < 4.2 | 1.3 |
| $\bar{4}\,4$ | < 2.5 | 2.9 |
| 5 | 10.5 | 10.4 |
| 6 | 7.2 | 6.4 |
| 7 | < 4.3 | 1.9 |
| 8 | < 4.4 | 1.5 |
| $\bar{9}$ | 4.1 | 4.3 |
| $3\,\bar{3}$ | 14.3 | 13.9 |
| 4 | 4.8 | 5.9 |
| 5 | 8.8 | 8.5 |
| 6 | 15.4 | 15.4 |
| 7 | < 4.3 | 3.8 |
| 8 | 4.5 | 4.3 |
| 9 | < 3.2 | 1.7 |
| $\bar{2}\,2$ | 24.1 | 23.3 |
| 3 | 20.5 | 20.2 |
| 4 | 5.5 | 6.0 |
| 5 | < 2.7 | 2.1 |
| 6 | 3.9 | 5.1 |
| 7 | 3.9 | 3.9 |
| $\bar{3}$ | < 4.1 | 2.4 |
| $1\,1$ | 13.7 | 13.7 |
| 2 | 6.5 | 7.5 |
| 3 | 9.7 | 10.0 |
| 4 | 15.4 | 16.3 |
| 5 | 4.2 | 4.7 |
| 6 | 3.8 | 3.8 |
| 7 | 4.6 | 4.4 |
| 8 | < 2.7 | 0.5 |

| $h\,k\,\ell$ | $G_o$ | $G_c$ |
|---|---|---|
| $0\,0\,1$ | < 2.0 | 0.5 |
| 2 | 10.2 | 11.4 |
| 3 | 3.5 | 3.9 |
| 4 | 10.2 | 11.2 |
| 5 | < 3.5 | 4.1 |
| 6 | < 4.4 | 3.1 |
| 7 | < 3.9 | 2.1 |
| $1\,1$ | 32.9 | 33.1 |
| 2 | 11.6 | 12.3 |
| 3 | 8.1 | 8.8 |
| 4 | 2.9 | 3.2 |
| 5 | 4.6 | 4.3 |
| 6 | 3.1 | 2.1 |
| 7 | 2.5 | 2.0 |
| $2\,2$ | 9.9 | 11.7 |
| 3 | 13.1 | 14.5 |
| 4 | < 4.4 | 1.9 |
| 5 | < 4.2 | 2.0 |
| 6 | 3.6 | 3.6 |
| $3\,3$ | 0.8 | 5.9 |
| 4 | 4.5 | 3.6 |
| 5 | < 3.5 | 2.0 |
| $\bar{4}$ | < 3.6 | 1.3 |
| $1\,\bar{1}\,4$ | 3.3 | 3.5 |
| 5 | < 2.7 | 1.1 |
| 6 | 2.7 | 3.0 |
| 7 | < 2.6 | 1.1 |
| 8 | < 2.6 | 2.9 |
| $\bar{9}\,2$ | < 2.3 | 2.4 |
| 3 | < 3.2 | 1.7 |
| 4 | 3.1 | 2.7 |
| 5 | 5.1 | 4.9 |
| 6 | 3.2 | 2.9 |
| 7 | < 3.2 | 2.4 |
| 8 | < 3.1 | 2.4 |
| $\bar{9}$ | < 2.0 | 1.1 |
| $8\,1$ | < 3.2 | 1.7 |
| 2 | 7.3 | 6.2 |
| 3 | 2.9 | 3.0 |
| 4 | < 3.3 | 1.5 |
| 5 | 3.8 | 3.6 |
| 6 | 4.1 | 3.9 |
| 7 | 3.7 | 2.3 |
| 8 | < 3.3 | 1.9 |
| 9 | < 3.0 | 2.3 |
| $\bar{7}\,1$ | 3.2 | 3.0 |
| 2 | 3.6 | 2.7 |
| 3 | 12.5 | 11.3 |
| 4 | < 3.1 | 0.8 |
| 5 | < 3.3 | 1.3 |
| 6 | 3.7 | 3.7 |
| 7 | 6.3 | 5.8 |
| 8 | 7.3 | 6.5 |
| 9 | < 3.0 | 0.9 |

| $h\,k\,\ell$ | $G_o$ | $G_c$ |
|---|---|---|
| $1\,\bar{6}\,1$ | 4.2 | 5.1 |
| 2 | 4.3 | 4.1 |
| 3 | 3.0 | 2.3 |
| 4 | 5.7 | 6.1 |
| 5 | 4.7 | 3.5 |
| 6 | < 3.1 | 1.5 |
| 7 | 3.2 | 2.5 |
| [illegible] | 4.7 | 3.9 |
| [illegible] | 3.3 | 2.8 |
| $\bar{5}\,1$ | [illegible] | 4.4 |
| 2 | [illegible] | 9.5 |
| 3 | 13.8 | 14.1 |
| 4 | 7.7 | 7.4 |
| 5 | 15.7 | 15.8 |
| 6 | 7.6 | 6.2 |
| 7 | < 3.3 | 1.2 |
| [illegible] | 3.2 | 3.7 |
| $\bar{9}$ | < 2.6 | 1.2 |
| $4\,1$ | 23.5 | 24.5 |
| 2 | 17.5 | 17.9 |
| 3 | 9.8 | 9.7 |
| [illegible] | 11.9 | 11.9 |
| 5 | 3.7 | 3.5 |
| 6 | 3.9 | 3.9 |
| 7 | < 3.3 | 1.4 |
| 8 | 4.9 | 3.9 |
| $\bar{9}$ | 2.1 | 2.3 |
| $3\,1$ | 4.2 | 4.4 |
| 2 | 34.2 | 32.5 |
| 3 | 15.5 | 13.7 |
| 4 | 7.5 | 7.1 |
| 5 | 2.8 | 2.9 |
| 6 | 3.0 | 2.6 |
| 7 | < 3.1 | 1.7 |
| 8 | 5.2 | 4.5 |
| $\bar{2}\,1$ | 16.9 | 17.2 |
| 2 | 28.7 | 29.6 |
| 3 | 6.9 | 6.4 |
| [illegible] | 11.3 | 13.4 |
| [illegible] | 9.3 | 10.1 |
| 6 | 6.3 | 6.5 |
| 7 | 3.9 | 3.5 |
| $\bar{8}$ | < 2.4 | 1.7 |
| $1\,1$ | < 2.7 | 0.5 |
| 2 | 29.3 | 29.9 |
| 3 | 12.5 | 14.4 |
| 4 | 2.8 | 2.7 |
| 5 | 10.4 | 11.1 |
| 6 | 5.9 | 5.8 |
| 7 | 4.9 | 4.9 |
| $1\,1$ | 10.3 | 11.5 |
| 2 | 12.9 | 13.5 |
| 3 | 2.9 | 3.0 |
| 4 | 4.2 | 3.6 |
| 5 | 5.0 | 4.3 |
| 6 | < 2.4 | 1.8 |

| $h\,k\,\ell$ | $G_o$ | $G_c$ |
|---|---|---|
| $1\,2\,2$ | 5.2 | 5.2 |
| 3 | < 3.1 | 1.6 |
| 4 | 7.7 | 7.5 |
| 5 | 2.6 | 1.7 |
| $3\,3$ | 3.3 | 2.3 |
| 4 | < 2.5 | 1.5 |
| $2\,\bar{10}\,3$ | < 7.1 | 1.1 |
| 4 | < 7.2 | 2.2 |
| 5 | < 7.3 | 2.5 |
| 6 | < 7.3 | 2.2 |
| 7 | < 7.2 | 0.6 |
| 8 | < 7.1 | 3.1 |
| $\bar{9}\,2$ | < 7.3 | 3.2 |
| 3 | < 7.2 | 2.1 |
| 4 | < 7.1 | 0.3 |
| 5 | < 7.0 | 3.4 |
| 6 | < 7.1 | 1.5 |
| 7 | < 7.2 | 3.7 |
| 8 | < 7.3 | 2.3 |
| $\bar{9}$ | < 7.2 | 2.5 |
| $\bar{1}\,2$ | < 7.2 | 1.9 |
| 3 | < 6.8 | 6.1 |
| 4 | < 6.6 | 1.7 |
| 5 | 10.2 | 9.0 |
| 6 | < 6.5 | 1.9 |
| 7 | < 7.0 | 2.5 |
| 8 | < 7.3 | 2.6 |
| $\bar{9}$ | < 7.1 | 2.6 |
| $\bar{7}\,2$ | < 6.3 | 3.0 |
| 3 | < 6.1 | 1.4 |
| 4 | 13.6 | 13.1 |
| 5 | 3.4 | 3.3 |
| 6 | < 6.9 | 2.9 |
| 7 | < 7.0 | 1.1 |
| 8 | < 7.2 | 1.5 |
| $\bar{9}$ | < 7.1 | 1.4 |
| $6\,2$ | < 4.7 | 0.2 |
| 3 | 10.7 | 10.3 |
| 4 | 8.1 | 7.2 |
| 5 | 4.7 | 4.7 |
| 6 | 9.1 | 9.9 |
| 7 | < 6.3 | 4.6 |
| 8 | < 7.2 | 2.1 |
| 9 | < 7.0 | 1.5 |
| $\bar{5}\,2$ | < 4.7 | 3.3 |
| 3 | 12.2 | 11.9 |
| 4 | 5.9 | 4.9 |
| 5 | 6.6 | 6.0 |
| 6 | < 5.9 | 5.5 |
| 7 | 9.7 | 9.3 |
| 8 | < 7.2 | 2.5 |
| 9 | < 6.8 | 2.1 |

| $h\,k\,\ell$ | $G_o$ | $G_c$ |
|---|---|---|
| $2\,\bar{4}\,2$ | 3.0 | 3.1 |
| 3 | 6.4 | 6.4 |
| 4 | 6.6 | 6.5 |
| 5 | 5.6 | 6.3 |
| 6 | 4.5 | 2.5 |
| 7 | < 7.1 | 4.3 |
| $\bar{8}$ | < 7.2 | 2.9 |
| $3\,\bar{3}$ | 7.2 | 6.9 |
| 3 | 12.7 | 12.9 |
| 4 | < 2.7 | 3.5 |
| 5 | 5.7 | 6.8 |
| 6 | < 4.5 | 0.7 |
| 7 | < 7.3 | 2.9 |
| $\bar{9}$ | < 7.0 | 2.7 |
| $2\,2$ | 20.5 | 20.9 |
| 3 | 10.2 | 11.3 |
| 4 | 9.8 | 10.2 |
| 5 | 5.2 | 6.4 |
| 6 | < 7.1 | 1.3 |
| 7 | < 7.3 | 2.7 |
| $\bar{8}$ | < 6.2 | 2.4 |
| $1\,2$ | < 2.6 | 1.0 |
| 3 | 2.5 | 3.2 |
| 4 | < 2.5 | 0.3 |
| 6 | 3.3 | 2.3 |
| 6 | 3.9 | 3.7 |
| $2\,2$ | < 6.5 | 4.4 |
| 3 | < 7.3 | 1.4 |
| 4 | < 7.3 | 2.2 |
| $3\,\bar{3}$ | < 7.4 | 1.1 |
| $3\,\bar{8}\,3$ | < 7.5 | 1.3 |
| 4 | < 5.5 | 2.2 |
| 5 | < 4.6 | 2.9 |
| $\bar{7}\,3$ | < 6.7 | 5.1 |
| 4 | < 4.9 | 1.4 |
| 5 | < 5.2 | 1.4 |
| $\bar{6}\,3$ | 6.3 | 5.3 |
| 4 | 11.1 | 12.0 |
| 5 | 6.6 | 4.1 |
| 6 | < 5.6 | 2.5 |
| $5\,3$ | < 7.4 | 1.5 |
| 4 | < 3.7 | 1.6 |
| 5 | < 4.9 | 4.7 |
| 6 | 5.5 | 4.7 |
| $\bar{4}\,3$ | 24.9 | 23.9 |
| 4 | 4.1 | 5.7 |
| 5 | < 4.2 | 4.7 |
| $\bar{6}$ | < 5.3 | 3.2 |
| $3\,3$ | < 3.7 | 0.3 |
| 4 | 7.0 | 8.3 |
| 5 | < 4.0 | 4.1 |

| $h\,k\,\ell$ | $G_o$ | $G_c$ |
|---|---|---|
| $3\,\bar{2}\,3$ | 11.5 | 11.9 |
| 4 | < 3.1 | 2.3 |
| 5 | < 7.1 | 4.3 |
| 6 | < 7.3 | 1.7 |
| $\bar{7}$ | < 6.6 | 1.3 |
| $1\,3$ | 3.1 | 3.7 |
| 4 | 5.9 | 5.1 |
| 5 | 3.3 | 3.3 |
| 6 | < 2.2 | 2.5 |
| $\bar{6}$ | < 4.2 | 0.5 |
| $7\,\bar{4}$ | < 7.2 | 0.3 |
| 5 | 9.4 | 9.7 |
| $\bar{6}\,4$ | < 6.6 | 2.6 |
| $\bar{5}$ | < 7.8 | 1.4 |
| $5\,4$ | < 6.5 | 1.5 |
| $\bar{7}$ | 7.4 | 7.6 |
| $4\,4$ | 11.1 | 11.7 |
| $\bar{5}$ | < 6.0 | 2.0 |
| $\bar{3}\,5$ | < 6.6 | 3.1 |
| $5\,\bar{4}\,5$ | < 7.1 | 2.1 |
| 5 | < 7.4 | 2.5 |
| $\bar{7}$ | < 6.8 | 2.3 |
| $5\,\bar{5}\,5$ | < 6.9 | 6.2 |
| $2\,5$ | < 6.8 | 4.1 |

* *Note.*— For the unresolved pairs ($2\bar{8}3$, $4\bar{6}5$), ($2\bar{7}6$, $3\bar{8}4$), and ($3\bar{5}5$, $4\bar{5}4$) the $G_o$ value given would be the observed amplitude if the other member of the pair were vanishingly weak.

The agreement residuals for the various proton arrangements range from $R=0{\cdot}087$ to 0·112, the corresponding range in the weighted sum of squares being $0{\cdot}99\times10^5$ to $2{\cdot}76\times10^5$. The improvement obtainable by introducing the more-suitable proton arrangements is probably meaningful, but the data do not distinguish among the arrangements giving the best agreement, namely: one ordered arrangement in $R\bar{3}$ (designated 2–I–4, 1–II–3 in a notation defined later), one in $R3$, and the proton-disordered arrangement. The lack of distinction among these is understandable, because all three look identical in the pseudo-structure in $R\bar{3}c$, which contributes most of the diffracted X-ray intensity. The reflections *hhl* with *l* odd provide here again a more sensitive basis for discrimination. It is found that the $R\bar{3}$ (2–I–4, 1–II–3) structure gives an agreement residual $R=0{\cdot}09$ for these reflections, whereas both the $R3$ structure and the disordered structure give $R=0{\cdot}18$. Since the (2–I–4, 1–II–3) ordered structure is strongly indicated by structural considerations, as discussed later, it was accepted as giving the correct proton arrangement and a final refinement of the oxygen parameters was carried out for this structure. The final agreement residual is $R=0{\cdot}080$ for the 152 observed reflections. Of the 126 unobserved reflections, only 2 calculate significantly greater than the limit of observation. The observed and calculated structure amplitudes for the final structure are listed in Table 2, and the atomic parameters are given in Table 3.

Table 3. *Atomic parameters in ice* II

| Atom | *x* | *y* | *z* | *B* (Å²) |
|---|---|---|---|---|
| $O_I$ | 0·273 | 0·024 | −0·146 | 1·93 ± 0·16 |
| $O_{II}$ | 0·478 | 0·750 | 0·332 | 1·78 |
| H(I2) | 0·165 | 0·069 | −0·190 | 2·1† |
| H(I4) | 0·413 | 0·205 | −0·003 | 2·1† |
| H(II1) | 0·719 | 0·401 | 0·395 | 2·1† |
| H(II3) | 0·741 | 0·203 | 0·360 | 2·1† |
| Perturbation vector: | | | | |
| **p** | 0·012 | 0·023 | 0·011 | |
| $O_{II}$* | 0·250 | −0·022 | −0·168 | |

† Assumed.

## Accuracy

The standard deviations of the oxygen coordinates in Table 3 are all very close to 0·0010, as derived from the full $6\times6$ least-squares matrix, which takes into account the considerable interaction between the oxygen atoms. The magnitude of the interaction can be judged from the complete variance–covariance matrix, given in Table 4. To evaluate the anisotropy of positional accuracy caused by the interaction, inverse variance–covariance matrices for the marginal densities of the $O_I$ and $O_{II}$ coordinates separately were obtained from the matrix in Table 4. On interchanging $x_{II}$ and $y_{II}$, these matrices are found to be quite similar, as expected on account of the pseudo-symmetry. The average between them is given in Table 3. Also listed are the principal axes for the quadratic form of this matrix, found by taking into account the skew coordinate system, and also the corresponding principal values expressed as principal standard deviations in units of the rhombohedral cell edge. The directions are appropriate to the position of $O_I$ as given in Table 3. The smallest principal standard deviation corresponds to the principal axis most nearly parallel to the perturbation vector (Table 3) by which the 'splitting' of the oxygen atoms in the pseudostructure is generated. This was surprising at first sight, but reflects the fact that in this direction the resolution of the atoms in the pseudostructure is actually the greatest, the 'split' atoms being com-

Table 4

Variance–covariance matrix for $O_I$ and $O_{II}$ coordinates

| | $x_I$ | $y_I$ | $z_I$ | $x_{II}$ | $y_{II}$ | $z_{II}$ |
|---|---|---|---|---|---|---|
| $x_I$ | 1·09 | 0·32 | 0·20 | 0·01 | −0·45 | 0·09 |
| $y_I$ | | 0·75 | 0·27 | −0·12 | −0·01 | 0·03 |
| $z_I$ | | | 1·14 | 0·01 | 0·06 | −0·59 |
| $x_{II}$ | | | | 0·91 | 0·53 | 0·51 |
| $y_{II}$ | | | | | 1·23 | 0·41 |
| $z_{II}$ | | | | | | 1·31 |

$\times10^{-6}$

Inverse variance–covariance matrix for marginal density of $O_I$ or $O_{II}$ coordinates alone

| | *x* | *y* | *z* |
|---|---|---|---|
| *x* | 1·08 | −0·50 | −0·10 |
| *y* | | 1·00 | −0·39 |
| *z* | | | 0·97 |

$\times10^6$

Principal standard deviations and principal axes

| *i* | $\sigma_i$ | $x_i$ | $y_i$ | $z_i$ |
|---|---|---|---|---|
| 1 | 0·0011 | 0·55 | 0·06 | −0·65 |
| 2 | 0·0008 | 0·66 | −0·42 | 0·52 |
| 3 | 0·0006 | 1·14 | 1·36 | 1·15 |

Table 5. *Oxygen coordination data for the actual structure* ($R\bar{3}$) *and the pseudo-structure* ($R\bar{3}c$)

| | $R\bar{3}$ | | $R\bar{3}c$ | $\sigma$ |
|---|---|---|---|---|
| *i* | I | II | 0 | |
| Distances (Å) | | | | |
| *i*–1 | 2·81 | 2·75 | 2·78 | ±0·012 |
| *i*–2 | 2·81 | 2·75 | 2·78 | ±0·012 |
| *i*–3 | 2·84 | | 2·84 | ±0·013 |
| *i*–4 | 2·80 | | 2·80 | ±0·007 |
| *i*–5 | 3·24 | | 3·24 | |
| Angles | | | | |
| 1–*i*–2 | 116* | 120° | 117·5° | ±0·3° |
| 1–*i*–3 | 85 | 99* | 92 | |
| 1–*i*–4 | 115·5* | 107·5* | 111·5 | |
| 2–*i*–3 | 126 | 125 | 125·5 | |
| 2–*i*–4 | 88* | 80 | 84 | |
| 3–*i*–4 | 129 | 127 | 128 | |

* Possible donor angles.

pletely superimposed as viewed in projection onto a plane perpendicular to the perturbation vector. It is seen that in spite of the interaction, $O_I$ is well resolved from the position of its companion 'half atom' in the $R\bar{3}c$ structure, for which the coordinates are given, under $O_{II}^*$, in Table 3.

Standard deviations for the O–O bond distances have been computed from the complete variance–covariance matrix, taking into account the correlation between the atomic positions. They are given in Table 5.

## Interpretation of the structure

Ice II can be described first in terms of a basic structure that is related in a certain way to Ice I, and then a relatively small but significant perturbation upon this basic structure.

The basic structure (or pseudo-structure) in $R\bar{3}c$ is related to ice I as follows. In the ice I structure (see *e.g.* the illustration in Pauling, 1960, p. 465) one can recognize hexagonal columns consisting of puckered six-rings of water molecules stacked one above the other. If these columns are detached from one another, moved relatively up and down parallel to the $c_H$-axis so as to give a rhombohedral stacking sequence for equivalent six-rings, and then rotated *ca.* 30° around their long ($c_H$) axes, they can be relinked together in a more tightly-fitting way than in ice I. This is the structure of ice II (Fig. 2). The scheme of cross-linking between the hexagonal columns causes the six-rings in each column to twist relative to one another through an angle of about 15°. This twist, plus a considerable flattening of the puckered six-rings, causes the $c_H$-axis to decrease from the value 7·36 Å in ice I to 6·25 Å in ice II. The coordination of the oxygen atoms is markedly distorted from the ideal tetrahedral one, as shown by the bond angles in Table 5. Each oxygen atom has four nearest neighbors at distances of $2{\cdot}80 \pm 0{\cdot}04$ Å. The distortion enables a next nearest neighbor at about 3·3 Å distance to be accommodated; this distance is the one between the atoms labelled I and II in Fig. 2.

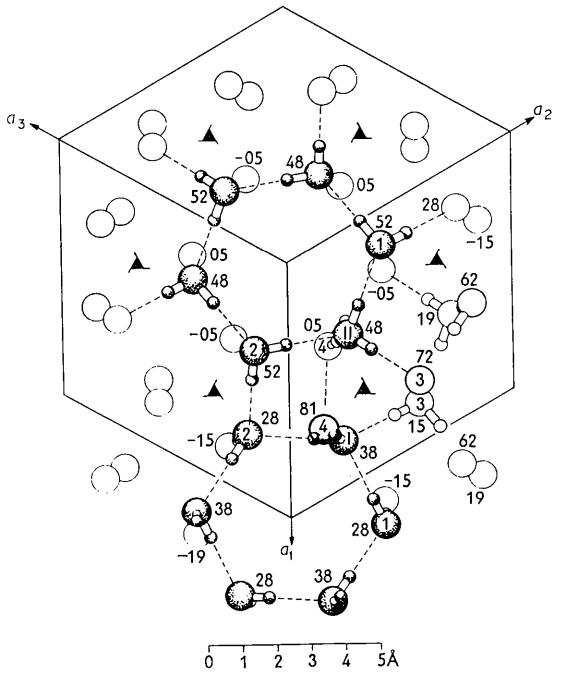


Fig. 2. The structure of ice II, viewed along the hexagonal $c_H$ axis. Heights of the atoms above a hexagonal (0001) plane are given in hundredths of the $c_H$ axis ($c_H = 6{\cdot}25$ Å). The rhombohedral unit cell is outlined. One six-ring of each of the two types, involving respectively $O_I$ and $O_{II}$, is emphasized, and the ordered water-molecule orientations in these rings are shown. Representative atoms $O_I$ and $O_{II}$ are labelled I and II respectively, and their nearest neighbors are numbered 1 through 4 in a scheme used in discussing the proton ordering. Hydrogen bonds are shown with a dashed line; the bonds linking up and down between the six-rings, to form the ice-I-like hexagonal columns, are omitted to avoid confusion.

The basic pseudo-structure is perturbed by 0·13 Å displacements of the oxygen atoms, eliminating the $c$ glide plane of the pseudo-structure and degrading the space group to $R\bar{3}$. The effect, though slight, is clearly visible in Fig. 2. It makes the six-ring involving $O_I$ become more strongly puckered, while the $O_{II}$ six-ring becomes almost flat.

It is contended that this perturbation is caused by an ordered arrangement of the protons in the structure. If the protons were in a disordered arrangement, as they are in ice I, the environments of all of the oxygen atoms would be on the average equivalent and the pseudo-structure in $R\bar{3}c$ would be retained. Any tendency for the bond distances or angles to assume values other than those imposed by the basic structure could not express itself in an ordered way; the only structural effect that could be detected would have the appearance of anisotropic thermal motion, representing the necessary short-range order. Such a situation is probably present in ice I (Peterson & Levy, 1957). It is assumed that there is here no effect on an intermolecular scale, analogous to the Jahn–Teller effect, that could lead to a spontaneous distortion of a disorder-averaged structure. The cause of the observed distortion must, then, be long-range ordering of the protons.

In the proton-ordered structure, the oxygen positions must conform to the symmetry of the proton arrangement. In the $R\bar{3}c$ structure two nearest neighbor oxygen atoms are related by a twofold axis. Since the O–O distance is long enough to require that the bond be asymmetric, the twofold axis must be dropped in the actual structure. This leads, as discussed previously, to assignment of space group $R\bar{3}$. The strong experimental confirmation of this space group *vis-à-vis* the possibility of space group $R32$ constitutes, conversely, further support for the interpretation of proton ordering.

The postulated twinning is a natural consequence of this interpretation. Within a basic $R\bar{3}c$ framework of oxygen positions, the two possible ways of ordering the protons (corresponding to opposite signs for the perturbation vector) are twinned counterparts. Since the proton ordering is energetically doubtless a small effect, it is to be expected that stacking faults in the proton ordering will arise, subdividing the basic single-crystal framework into twinned domains.

### Assignment of proton positions

From the detailed features of oxygen coordination in the structure (Table 5) it is possible to infer the positions of the protons. The bond distances are of no direct help, because every H-bond must involve a proton at one end or the other. It is the bond angles that provide the necessary clues, since, of the six bond angles at each oxygen atom, only one can be occupied by the H–O–H angle of the water molecule at that site.

The tendency for the water molecule to form bonds at tetrahedral angles, as shown in ice I and in crystalline hydrates (Wells, 1962; Baur, 1962; Clark, 1963), indicates that the hydrogen bond energy has significant dependence on bond angle. The energy dependence results from bending of the H-bonds: it is known that the water molecule in crystalline hydrates is little distorted from its configuration in the vapor (McGrath & Silvidi, 1961; Chidambaram, 1962). In most hydrates, the O · · · O · · · O angles presented to the water molecules are prevented by other steric requirements from adjusting to the angle favored by the water molecules, so that deviations of donor O—H by as much as 15° from the O · · · O bond occur.

In ice II, there is freedom for the bond angles to adjust without essential alteration of the bond distances, as indicated by comparison of bond distances in the pseudo-structure and the actual structure. We therefore assume that the structure distorts in such a way as to bring the O · · · O · · · O angles presented to the H–O–H groups (donor angles) closer to the angle for which H-bond energy is a maximum. The favored angle might reasonably be taken either as 104·6°, the H–O–H angle of the isolated water molecule (Darling & Dennison, 1940), or 109·5°, the tetrahedral coordination angle in ice I. Since angles reasonably near these values are present, the angles that deviate greatly may be eliminated, leaving for consideration as donor angles only the angles marked with an asterisk in Table 5. The seemingly most favorable pair of angles* is (1–I–4, 1–II–4) but this must be ruled out because it makes the two oxygen atoms equivalent and also violates the restriction that there be only one proton per H-bond. The pair (1–I–4, 1–II–3) avoids this difficulty, but presents another: the angle 1–II–3 is improved by the distortion from the pseudo-structure, but the angle 1–I–4 is worsened. For (2–I–4, 1–II–3), on the other hand, both angles are improved by the distortion. The angle 1–I–2 cannot be used for a structure in space group $R\bar{3}$, but it can be used in $R3$; however, this then requires use of 3–I–4, which is one of the worst angles of the group.

It might appear from the bond angles that the proton arrangement (1–I–4, 1–II–3) would have lower total energy (higher H-bond energy) than (2–I–4, 1–II–3) and should therefore be preferred. However, three features of the structure argue in favor of (2–I–4, 1–II–3).

Consider first the perturbation by which the $R\bar{3}c$ pseudo-structure distorts into the actual structure. The data in Table 5 show that a considerable distortion from the pseudo-structure is possible without essential change in any of the O · · · O bond distances. In fact it can be shown, and also visualized from Fig. 2, that the structure is free to distort in ways quite different from the perturbation actually observed, still without sensibly changing the O · · · O distances. Consider the perturbation vector applied at the atom labelled II in Fig. 2. Any perturbation vector lying approximately in a plane parallel to the $c_H$ axis and containing the II–4 bond direction has the above property. What then determines the direction of the perturbation vector in this plane?

Let the direction of the perturbation vector be defined by the angle $\xi$ that it makes with the $c_H$ axis, $\xi$ being measured positive in the direction from $+c_H$ toward the O–O vector from 4 to II (Fig. 2). The changes produced in the various bond angles by the distortion can be calculated in terms of $\xi$ and the length $p$ of the perturbation vector. To first order in $p$ they are as follows

$$\begin{aligned} \Delta(1\text{–II–}3) &= \quad (22\cos\xi + 51\sin\xi)p \\ \Delta(2\text{–I–}4) &= \quad (38{\cdot}4\cos\xi + 2{\cdot}7\sin\xi)p \\ \Delta(1\text{–I–}4) &= -(38{\cdot}4\cos\xi + 2{\cdot}7\sin\xi)p \end{aligned}$$

where $p$ is taken in Å and the angle changes are obtained in degrees.

If now the protons of the water molecules went into the arrangement (1–I–4, 1–II–3), one could expect the $R\bar{3}c$ structure to distort in such a way that the original angles 1–0–4 and 1–0–3 become modified so as to minimize the quantity

* The angles are labelled in accordance with the scheme indicated in Fig. 2. The nearest-neighbor oxygen atoms of $O_I$ and $O_{II}$ are numbered from 1 to 4 in a way that would be symmetry-equivalent for $O_I$ and $O_{II}$ if a c-glide plane were actually operative. The proton positions are designated according to this same scheme; thus (1–I–4) designates a water molecule at $O_I$ oriented so as to donate its protons to neighbors 1 and 4 of $O_I$. The angles in the undistorted pseudo-structure are designated by replacing the I or II (which are here equivalent) by 0.

$$[(1\text{–}0\text{–}4)+\Delta(1\text{–}I\text{–}4)-104{\cdot}6]^2 + [(1\text{–}0\text{–}3)+\Delta(1\text{–}II\text{–}3)-104{\cdot}6]^2$$

whereas for arrangement (2–I–4, 1–II–3) the distortion should try to minimize

$$[(2\text{–}0\text{–}4)+\Delta(2\text{–}I\text{–}4)-104{\cdot}6]^2 + [(1\text{–}0\text{–}3)+\Delta(1\text{–}II\text{–}3)-104{\cdot}6]^2.$$

By minimizing these quantities with respect to $\xi$, for fixed $p$ (assumed small), we can predict what the perturbation direction $\xi$ should be for the two proton arrangements. The predicted angles are $\xi=90°$ for (1–I–4, 1–II–3) and $\xi=39°$ for (2–I–4, 1–II–3). The observed angle is $\xi=42{\cdot}6\pm2{\cdot}7°$. The distortion is therefore appropriate to the (2–I–4, 1–II–3) structure only.

In more general terms, the (1–I–4, 1–II–3) structure would seem to be unfavorable to the existence of long-range proton ordering, regardless of whether or not the 'most appropriate' distortion of the structure were achieved. If the angles 1–I–4 and 1–II–4 were available for occupancy by H–O–H, it appears that (1–II–4) would be at least as favored if not more so than (1–I–4); this would tend to upset the ordering in the six-ring involving $O_{II}$, and thus cause a breakdown of long range order in the crystal. It seems that the existence of an ordered arrangement of energetically well-favored angles for H–O–H occupancy is essential to achieving long-range proton ordering. Its absence is probably responsible for the failure of ice I to achieve proton ordering at low temperature (Pauling, 1960, pp. 464–468).

We have so far considered the proton ordering in terms of the donor hydrogen bonds made by each water molecule. The acceptor relationships appear to be important also. In terms of the usually postulated tetrahedral character of the water molecule, the acceptor bond orientations indicated by the angles in Table 5 look rather unfavorable. For structure (2–II–4, 1–I–3), the acceptor–acceptor bond angle is the smallest O···O···O angle at both $O_I$ and $O_{II}$, being much below the tetrahedral value. The distortion of the coordination polyhedra from ideal tetrahedral configuration is so great that there is no possibility of achieving a tetrahedral acceptor orientation in relation to donor protons ordered in a reasonably favorable way. It is therefore necessary to seek a less restrictive criterion for favorable acceptor-bond orientation.

A necessary but not sufficient condition for tetrahedral acceptor-bond orientation is that these bonds should lie in the symmetry plane that bisects the H–O–H angle of the water molecule. The structure of ice II allows this condition to be satisfied rather well for water molecules in the arrangement (2–I–4, 1–II–3), but not for the alternative arrangements. This is shown by determining, for each possible water molecule orientation, the angle $\Gamma$ between the acceptor plane (O···O···O plane defined by oxygen atoms from which H-bonds are accepted at the given water molecule) and the H–O–H bisecting plane, it being assumed that the protons orient themselves symmetrically with respect to the O···O···O angle to which they donate H-bonds (donor angle). Acceptor-plane misorientation angles $\Gamma$ are given in Table 6, first for the $R\bar{3}c$ structure, and then in more detail for the more favorable angles in the actual structure. The (1–I–4) orientation, considered as possible in terms of the size of the donor angle, is seen to be markedly unfavorable in relation to its acceptor plane.

Table 6. *Acceptor-plane misorientation angle $\Gamma$*

| Structure | Donor angle | Acceptor angle | $\Gamma$ |
|---|---|---|---|
| $R\bar{3}c$ | 2–0–3 | 1–0–4 | 25° |
| $R\bar{3}c$ | 1–0–4 | 2–0–3 | 24 |
| $R\bar{3}c$ | 3–0–4 | 1–0–2 | 23 |
| $R\bar{3}c$ | 1–0–2 | 3–0–4 | 20 |
| $R\bar{3}c$ | 1–0–3 | 2–0–4 | 12 |
| $R\bar{3}c$ | 2–0–4 | 1–0–3 | 6 |
| $R3$ | 1–I–4 | 2–I–3 | 24·5 |
| $R\bar{3}$ | 1–II–4 | 2–II–3 | 24 |
| $R\bar{3}$ | 1–I–3 | 2–I–4 | 11 |
| $R\bar{3}$ | 1–II–3 | 2–II–4 | 12·5 |
| $R\bar{3}$ | 2–I–4 | 1–I–3 | 2 |
| $R\bar{3}$ | 2–II–4 | 1–II–3 | 9·5 |

A complete picture of acceptor-bond orientation in relation to bisecting plane is obtained in stereographic projection (Fig. 3). The acceptor-bond misorientation can be specified in terms of two angles $\omega$ and $\varphi$, $\omega$ measuring the angular departure from the bisecting plane, and $\varphi$ the azimuthal orientation relative to the 'negative pole' of the water molecule (the axis bisecting the H–O–H angle, on the side away from the protons). In Table 7 the misorientation parameters for the H-bonds in structures (2–I–4, 1–II–3) and (1–I–4, 1–II–3) are given. Donor misorientation is specified in terms of the angle $\Omega=\frac{1}{2}(\theta_D-104{\cdot}6°)$, $\theta_D$ being the donor angle. The large increases in $\omega$ for bonds I–2 and II–3 in structure (1–I–4, 1–II–3), in comparison to the smaller increases in $\Omega$ for (2–I–4, 1–II–3), tend to favor selection of the latter structure.

Table 7. *Bond-strain parameters*

| | | (2–I–4, 1–II–3) | | | (1–I–4, 1–II–3) | | |
|---|---|---|---|---|---|---|---|
| Bond | $d$ (Å) | $\Omega$ | $\omega$ | $\varphi$ | $\Omega$ | $\omega$ | $\varphi$ |
| I–2 | 2·81 | 8° | 0·5° | 53·5 | 5·5° | 15° | 67° |
| I–4 | 2·80 | 8 | 11·5 | 45 | 5·5 | 11·5 | 45 |
| II–1 | 2·75 | 2·5 | 3·5 | 35 | 2·5 | 3·5 | 35 |
| II–3 | 2·84 | 2·5 | 2 | 32 | 2·5 | 24 | 56 |

The consistency of the structural indications discussed above supports the following interpretation

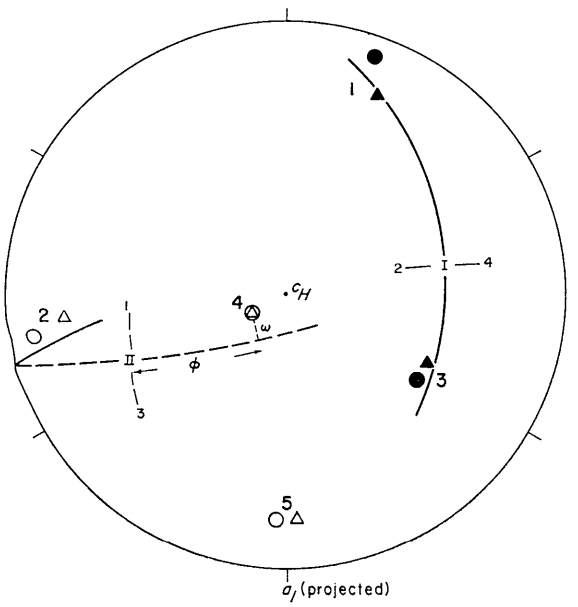


Triangles: neighbors to $O_I$; circles: neighbors to $O_{II}$. Filled symbols: upper hemisphere; open symbols: lower hemisphere.

Fig. 3. Stereographic projection of the coordination polyhedra around $O_I$ (triangles) and $O_{II}$ (circles). The neighbors are numbered in conformity with Fig. 2; 5 is the next-nearest neighbor. The orientation of the diagram conforms to $O_{II}$ in Fig. 2; for $O_I$, the orientation corresponds to the twinned counterpart of Fig. 2. The donor-bisecting planes for donor angles 2–I–4 and 1–II–3 are shown, solid on the upper hemisphere, dashed below. The points I and II are the 'negative poles' of the respective water molecules. Representative acceptor misorientation angles $\omega$ and $\varphi$ are labelled.

of the ice II structure: (1) The protons are ordered in the scheme (2–I–4, 1–II–3). (2) Both donor and acceptor relationships are important in achieving the proton ordering. (3) The criterion for favorable acceptor bonds is that the bonds lie in or near the H–O–H bisecting plane ($\omega \simeq 0$), without regard to their precise orientation within this plane ($\varphi$ value). This criterion corresponds to the electronic structure of the water molecule presented by Lennard-Jones & Pople (1951, p. 157), in which a 'ridge' of high electron density follows the negative side of the H–O–H bisecting plane, the maximum density being at the 'negative pole' of the molecule. The presence in ice II of acceptor–acceptor angles rather smaller than tetrahedral is in accord with this, and also with arguments of the type given by Pauling (1958) for the plausibility of linear N–H $\cdots$ O=C bonds in polypeptides, and with the observation by Clark (1963) of the frequent occurrence of threefold coordination of water molecules in organic hydrates.

The proton-ordering scheme derived by structural arguments is supported by the X-ray data, although the support provided can necessarily have only marginal statistical significance. It is hoped to carry out a neutron diffraction study of ice II to test experimentally the arguments presented.

## Thermodynamic considerations

The ordering of water molecule orientations in ice II is reasonable in terms of the stability field of this phase in relation to other forms of ice (Fig. 1). The impossibility of superheating II into the fields of stability of III or V (Bridgman, 1912, p. 530) which contrasts with the readily achieved supercooling of III and V into the field of II, suggests a 'melting' of the proton ordering analogous to melting of the oxygen framework that occurs at the solid-liquid transition, which shows this same type of supercooling *versus* superheating relationship for all of the solid phases (except II). The proton 'melting' cannot take place within the oxygen framework of ice II because of the energetic unfavorability of most of the possible water molecule orientations in the structure; hence the oxygen framework changes to that of ice III (in which the protons are probably disordered).

It seems that the proton-ordering transformations are particularly difficult to achieve. Bridgman (1912, p. 494) found that once II is completely transformed to III, it is very difficult to retransform directly to II, an exception to the typical 'memory' phenomenon exhibited in the interconversion of ice polymorphs (Bridgman, 1912, p. 532). Likewise, II cannot be formed initially from I without cooling to about $-70$ °C, far below the actual upper limit of ice II stability.

As determined by Bridgman's measurements (1912, p. 492), the entropy of ice II is 0·77 cal. mole$^{-1}$.deg$^{-1}$ less than that of ice I, over the temperature range from $-34$ °C to $-75$ °C. This value is close to the residual entropy of ice I, 0·82 cal. mole$^{-1}$.deg$^{-1}$ as measured by Giauque & Ashley (1933), or 0·81 as calculated by Pauling (1935) on the basis of proton disorder. The measured $\Delta S$ value can thus represent directly the proton ordering in ice II, provided that the difference in lattice-vibrational entropy between I and II is small. There is no direct evidence for this, but it seems likely, on the basis of comparison of relative entropies of the various ice polymorphs (Table 8). The entropy of ice II is less than that of the other ice phases by amounts an order of magnitude larger than the entropy differences among the other phases themselves, it being therefore also likely that these other forms are all proton-disordered.

Considering the rather large distortions from an 'ideal' tetrahedral environment for the water molecules in ice II, it is remarkable that the internal energy of this phase is so nearly equal to that of ice I, especially by comparison with the other high-pressure forms of ice (Table 9). Because in ice II the average donor angle is only 94·5°, the idea presents itself that the

Table 8. *Entropy changes for ice–ice transitions*

| From | II | II | II | I | III | V | IV | VI |
|---|---|---|---|---|---|---|---|---|
| To | I | III | V | III | V | VI | VI | VII |
| $\Delta S$ | +0·8 | +1·0 | +1·0 | +0·08 | −0·06 | +0·05 | −0·13 | +0·05 |

Units of cal.mole$^{-1}$.deg$^{-1}$. Values are averages over the respective equilibrium curves, from determinations by Bridgman (1912, 1935, 1937). Value involving ice IV is for $D_2O$.

energetically most-favored H-bond donor angle of the water molecule may for some reason be smaller than the H–O–H angle of the free water molecule. However, a case cannot be made for this idea, because of the considerable stabilization provided by the increased van der Waals interaction in ice II.

Table 9. *Energy of ice polymorphs relative to ice I*

| Ice | II | III | IV | V | VI | VII |
|---|---|---|---|---|---|---|
| $E-E(I)$ | 0·01 | 0·25 | 0·38 | 0·34 | 0·42 | 0·95 |

Units of kcal.mole$^{-1}$. Values are approximate, based on $\Delta E$ determinations by Bridgman (1912, 1935, 1937); $\partial E/\partial P$ and $\partial E/\partial T$ for the individual phases have been neglected.

The energy difference between ice I and ice II can be estimated by considering (1) H-bond strain energy, (2) van der Waals energy of non-nearest neighbors, and (3) electrostatic interaction of non-nearest neighbors. Of these, (2) is the most reliably estimated, (3) requires extensive calculations beyond the scope of this paper, and will not be considered here. The H-bond strain energy (1) involves bond-length strain (which includes the energy of repulsive forces and van der Waals attractive forces for nearest neighbors) and also bond-angle strain, represented by the angular misorientation parameters in Table 7.

To the extent that bond-length and bond-angle strains are independent, the bond-length strain energy can be estimated in the way given by Pauling (1960, p. 453). The bond-angle strain energy will be assumed to have the form

$$\hat{E} = \varkappa(\Omega^2 + \nu\omega^2) \qquad (1)$$

where $\varkappa$ and $\nu$ are constants, $\nu$ defining the relative energy contributions of acceptor misorientation and donor misorientation. Dependence of this type on $\Omega$ has been introduced by several previous authors (Table 10). The proposed dependence on $\omega$ is based on the structural indication in ice II that the acceptor orientation is sensitive to $\omega$ but not to $\varphi$. Pople (1950) used a relation like (1), but took for the acceptor misorientation the departure angle from *tetrahedral* orientation relative to the water molecule; he also assumed in effect $\nu=1$. Quoted values of $\varkappa$ are listed in Table 10; the value $\varkappa=6$ cal. mole$^{-1}$.deg$^{-2}$, which will be used here, is not likely to be in error by more than a factor of 2.

The van der Waals energy of non-nearest neighbors can be estimated by the method used by Pauling & Simonetta (1952, p. 31; see also Pauling, 1961), which for a pair of water molecules at distance $r$ gives an energy

$$E_{vW} = -1{\cdot}67(d_0/r)^6 \text{ kcal.mole}^{-1} \qquad (2)$$

where $d_0=2{\cdot}76$ Å. We obtain the van der Waals energy of ice I by summing the individual contributions for O–O distances out to 6·7 Å, and carrying out an integration beyond; for ice II the integration is started at 6·0 Å.

The estimated energy contributions are given in Table 11. The calculated energy of ice II is too low, in spite of the significant amount of bond-strain energy. This is because the denser packing of ice II, which involves eight O–O distances in the range 3·24 to 3·92 Å and five more between 4·24 and 4·47 Å, gives a much higher van der Waals energy than the open structure of ice I, with twelve next-nearest neighbors at 4·50 Å and one at 4·60 Å. The calculated

Table 10. *Values of $\varkappa$ in equation* (1)

| Source | $\varkappa$ (cal.mole$^{-1}$.deg$^{-2}$) | Method |
|---|---|---|
| Chidambaram (1962) | 8·8 | Theoretical* after Lippincott & Schroeder (1955) |
| Cross *et al.* (1937) | 4·2 | Raman spectrum of water |
| Pauling & Corey (1954) | 7·3 | Empirical |
| Pimentel & McClellan (1960) | 4·9 | Libration frequency $\nu_R$ in ice |
| Pimentel & McClellan (1960) | 1·1 | Theoretical (electrostatic model) |
| Pople (1950) | 8·2 | Radial distribution curve for water |
| Pople (1950) | 8·2 | Theoretical (electrostatic model) |
| Present work† | 2·2 | Bending frequency $\nu_2$ in ice |

* The bending energy was calculated for $\Omega=2{\cdot}5°$ only, the dependence on $\Omega$ not being given explicitly.

† Calculated from spectroscopic data from Ockman (1958), by assuming that the acceptor oxygen is rigidly fixed during the bending vibration. This improbable assumption is probably responsible for the discrepancy between $\varkappa$ values obtained from $\nu_R$ and $\nu_2$, which has been noted by Pimentel & McClellan (1960, p. 127). An interpretation that does not require such a low value of $\varkappa$ is given by Zimmerman & Pimentel (1962, p. 735).

energy difference could be made to agree with experiment by taking $\varkappa = 9$ cal. mole$^{-1}$.deg$^{-2}$.

Table 11. *Calculated energy contributions for ice I and II*

| | I | II |
|---|---|---|
| | | (kcal.mole$^{-1}$) |
| Bond-length strain | 0 | 0·04 |
| Bond-angle strain | | |
| Donor misorientation | 0·07 | 0·42 |
| Acceptor misorientation ($\nu = 1$) | 0 | 0·39 |
| Van der Waals energy | −0·96 | −2·17 |
| Totals | −0·9 | −1·3 |

Calculated $E(\text{II})-E(\text{I}) = -0{\cdot}4$ kcal.mole$^{-1}$
Measured (Bridgman, 1912) $= +0{\cdot}01$

To compute the acceptor energy contribution on the basis of deviation from tetrahedral orientation, as done by Pople (1950), we must add to equation (1) a term $\varkappa\nu(\varphi - 54{\cdot}7°)^2$. From the data in Table 7, the resulting additional contribution (for $\nu = 1$) to the energy of ice II is +3·1 kcal.mole$^{-1}$, much too large to be compatible with the observed energy. This argues against the concept of the tetrahedral water molecule in its elementary form, and in favor of the interpretation presented here, in which the acceptor energy is independent of $\varphi$.

From Table 7 it is found, on the basis of equation (1), that water-molecule orientation (2–I–4) will be favored energetically over (1–I–4) provided that $\nu > 0{\cdot}1$.

On the same basis, the energy of a hypothetical, completely proton-disordered form of ice II can be estimated. From data of the kind in Table 7, and assuming $\nu = 1$, the disordering energy is found to be +3·0 kcal.mole$^{-1}$, so large as to prevent a transition to the disordered form.

The bond lengths in ice II do not conform in a simple way to the bond strength criterion given by equation (1), as shown by the data in Table 7. The longest bond, $2{\cdot}84 \pm 0{\cdot}01_3$ Å, and the shortest, $2{\cdot}75 \pm 0{\cdot}01_2$ Å, ought to correspond to almost the same strength in terms of bond-bending strain. Evidently the bond lengths are affected by other factors. The long bond is the one between the ice-I-like hexagonal columns of six-rings, and it could shorten without altering any of the other bond lengths if the columns were to come closer together by contraction of the $a_H$ axis. However, the non-bonded distance of 3·24 Å would be shortened by the full amount of the contraction. Apparently a repulsion becoming effective at this distance prevents shortening of the 2·84 Å bond length.

It is worth noting that the favorable energetic relations involving the proton ordering peculiar to ice II are probably responsible for the fact that this structure, unlike the other known ice structures, has no analog among the polymorphs of silica so far discovered.

*Note added in proof.* — Recently Bertie & Whalley (1964) have published spectroscopic data which they interpret as indicating proton ordering in ice II and ice III, although it is not clear whether long-range or short-range order is contemplated. The evidence discussed here casts doubt on interpretation in terms of long-range proton order because crystallographic and thermodynamic data indicate a sharp distinction between ice III (disordered) and ice II (ordered). The crystallographic results for ice II imply that the acceptor relationship must be taken into account in interpreting the spectral bands that involve H-bond bending. The bending anisotropy should lead, for example, to a splitting of the libration modes, which are usually assigned a single frequency. This may help to explain the two libration frequencies of about 800 cm$^{-1}$ and 500 cm$^{-1}$ found for HDO by Bertie & Whalley (1964) and it may contribute to the breadth of the $\nu_R$ band in the pure $H_2O$ and $D_2O$ ices. If these interpretations are correct, the spectroscopic data constitute additional evidence for an appreciable value for the parameter $\nu$ in equation (1) above. In another recent paper Bertie, Calvert & Whalley (1964, p. 1377) report that ice II has a low dielectric constant and no detectable dielectric relaxation, in contrast to ices I, III, V, and VI. This provides striking confirmation of the interpretations of proton order *versus* disorder presented in the present paper.

It is a pleasure to acknowledge the important contribution to this work of Carolyn Knobler, who read and reduced the X-ray intensities and helped in various other ways. R. E. Marsh kindly provided his triclinic least-squares program, and gave helpful discussion and advice. I am indebted to Linus Pauling for many discussions and valuable ideas, and for suggesting the investigation originally. The work was supported by grants G-4537 and G-19769 from the National Science Foundation.

## References

Baur, W. H. (1962). *Acta Cryst.* **15**, 815.
Bernal, J. D. & Fowler, R. H. (1933). *J. Chem. Phys.* **1**, 515.
Bertie, J. E., Calvert, L. D. & Whalley, E. (1963). *J. Chem. Phys.* **38**, 840.
Bertie. J. E., Calvert, L. D. & Whalley, E. (1964). *Canad. J. Chem.* **42**, 1373.
Bertie, J. E. & Whalley, E. (1964). *J. Chem. Phys.* **40**, 1646.
Bjerrum, N. (1952). *Science*, **115**, 385.
Bode, H. & Teufer, G. (1955). *Acta Cryst.* **8**, 611.
Bridgman, P. W. (1912). *Proc. Amer. Acad.* **47**, 441.
Bridgman, P. W. (1935). *J. Chem. Phys.* **3**, 597.
Bridgman, P. W. (1937). *J. Chem. Phys.* **5**, 964.
Chidambaram, R. (1962). *J. Chem. Phys.* **36**, 2361.
Clark, J. R. (1963). *Aust. J. Pure Appl. Phys.* **13**, 50.

CROSS, P. C., BURNHAM, J. & LEIGHTON, P. A. (1937). *J. Amer. Chem. Soc.* **59**, 1134.
DARLING, B. T. & DENNISON, D. M. (1940). *Phys. Rev.* **57**, 218.
GIAUQUE, W. F. & ASHLEY, M. (1933). *Phys. Rev.* **43**, 81.
KAMB, B. & DATTA, S. K. (1960*a*). *Nature, Lond.* **187**, 140.
KAMB, B. & DATTA, S. K. (1960*b*). *Acta Cryst.* **13**, 1029.
KAMB, B. & DATTA, S. K. (1960*c*). Unpublished manuscript.
*International Tables for X-ray Crystallography* (1959). Vol. II. Birmingham: Kynoch Press.
LENNARD-JONES, J. & POPLE, J. A. (1951). *Proc. Roy. Soc.* A, **205**, 155.
LIPPINCOTT, E. R. & SCHROEDER, R. (1955). *J. Chem. Phys.* **23**, 1099.
LONSDALE, K. (1958). *Proc. Roy. Soc.* A, **247**, 424.
MCFARLAN, R. L. (1936*a*). *J. Chem. Phys.* **4**, 60.
MCFARLAN, R. L. (1936*b*). *Rev. Sci. Instrum.* **7**, 82.
MCGRATH, J. W. & SILVIDI, A. A. (1961). *J. Chem. Phys.* **34**, 322.
OCKMAN, N. (1958). *Advanc. Phys.* **7**, 199.
OWSTON, P. G. (1958). *Advanc. Phys.* **7**, 171.
PAULING, L. (1935). *J. Amer. Chem. Soc.* **57**, 2680.
PAULING, L. (1958). In *Symposium on Protein Structure*, Ed. NEUBERGER, A. p. 17. London: Methuen.
PAULING, L. (1960). *The Nature of the Chemical Bond.* Ithaca: Cornell Univ. Press.
PAULING, L. (1961). *Science*, **134**, 15.
PAULING, L. & COREY, R. B. (1954). *Fortschr. Chem. org. Naturst.* **11**, 180.
PAULING, L. & SIMONETTA, M. (1952). *J. Chem. Phys.* **20**, 29.
PETERSON, S. W. & LEVY, H. A. (1957). *Acta Cryst.* **10**, 70.
PIMENTEL, G. C. & MCCLELLAN, A. L. (1960). *The Hydrogen Bond.* San Francisco: Freeman.
PITZER, K. S. & POLISSAR, J. (1956). *J. Phys. Chem.* **60**, 1140.
POPLE, J. A. (1950). *Proc. Roy. Soc.* A, **205**, 163.
WELLS, A. F. (1962). *Structural Inorganic Chemistry* (3d ed.): Oxford.
ZIMMERMAN, R. & PIMENTEL, G. C. (1962). In *Advances in Molecular Spectroscopy.* Ed. MANGINI, A. p. 726. New York: Pergamon Press.

*Acta Cryst.* (1964). **17**, 1449

# The Structures of Some Inorganic Cyanamides. I. Preparation of Single Crystals and Preliminary Studies

BY K. M. ADAMS*, M. J. COOPER*† AND M. J. SOLE‡§
*Cavendish Laboratory, Cambridge, England*

(*Received* 26 *November* 1963)

The preparation of single crystals of sodium, thallous, silver and lead cyanamides is described. Preliminary crystallographic data on these compounds are reported.

## Introduction

A detailed study has recently been made of the physical properties, molecular structure and thermal and radiation stability of a number of inorganic cyanamides (Sole, 1963; Sole & Yoffe, 1964). Crystallographic studies of these compounds have therefore been undertaken in order to correlate the physical properties with the detailed crystal structures. The compounds investigated, namely sodium, thallous, silver and lead cyanamides, are fairly readily available as polycrystalline or amorphous powders and methods for their preparation in this form have been described previously (Shushunov & Pavlov, 1955; Deb & Yoffe, 1959; Bolis-Caunella & Costa, 1953). However the single crystals required for the above investigations are difficult to prepare and the methods used are therefore described in some detail in this paper. Preliminary crystallographic data are also reported.

## Sodium cyanamide

An attempt to prepare sodium cyanamide by the method of Shushunov & Pavlov (1955) was unsuccessful and from infrared and X-ray analyses the product appeared to be mainly sodium acid cyanamide. Accordingly sodium cyanamide in the form of fused ingots was obtained from Bios Laboratories Incor-

* Crystallographic Laboratory.
† Formerly Mullard Research Fellow, Downing College, Cambridge. Present address: Brookhaven National Laboratory, Long Island, New York, U.S.A.
‡ Laboratory of Physics and Chemistry of Solids.
§ Present address: Atomic Energy Board, Pretoria, South Africa.